Lifeng Ma
S&V Lab,
Department of Engineering Mechanics,
Xi'an Jiaotong University,
710049, China

Alexander M. Korsunsky
Department of Engineering Science,
University of Oxford,
Oxford OX1 3PJ, UK

Robert M. McMeeking
Department of Mechanical Engineering and
Materials Department,
University of California,
Santa Barbara, CA 93106;
School of Engineering,
University of Aberdeen,
Aberdeen AB24 3UE, UK;
INM - Leibniz Institute for New Materials,
Campus D2 2,
66123 Saarbrücken, Germany

Fundamental Formulation for Transformation Toughening in Anisotropic Solids

In this paper the problem of transformation toughening in anisotropic solids is addressed in the framework of Stroh formalism. The fundamental solutions for a transformed strain nucleus located in an infinite anisotropic elastic plane are derived first. Furthermore, the solution for the interaction of a crack tip with a residual strain nucleus is obtained. On the basis of these expressions, fundamental formulations are presented for the toughening arising from transformations using the Green's function method. Finally, a representative example is studied to demonstrate the relevance of the fundamental formulation.
[DOI: 10.1115/1.4023476]

1 Introduction

Phase transformations in ceramics such as martensitic metamorphoses can involve spontaneous strain, and ferroelastic response occurs when such spontaneous strains are modified by, for example, exchange of twin variants (see, e.g., [1–13]). Such permanent strain, if heterogeneous, gives rise to self-equilibrating residual stresses within the object. These transformation stresses have a significant influence on the deformation and apparent toughness of engineering ceramics. In the case of martensitic transformation, experiments reveal that toughening is associated with a stress-induced phase transformation in the vicinity of the crack tip. When the stresses in the region near the crack tip reach a critical value, the transformation occurs, typically from tetragonal to monoclinic in zirconia ceramics, and is accompanied by a volume increment of 4% and a shear strain of 16%, the latter largely nullified by twinning. These strains induce constraint stresses, and the crack tip stress intensity factor is reduced, usually after some stable crack growth. Therefore, the fracture toughness of the ceramic is effectively enhanced since it now takes higher applied loads to raise the stress intensity factor back to the critical level required to cause continued crack propagation. In contrast to the martensitic case, ferroelastic transformations typically involve only the deviatoric component of the permanent strain. Ferroelastic toughening is attributed to domain switching of twins in the crack front and in the crack wake, inducing stress intensity factor reduction (see, e.g., [14–19]).

In order to explore the potential toughness benefits of phase transformation and ferroelastic behavior, much effort has been devoted to modeling in this field. Three main approaches to simulating transformation and ferroelastic toughening have been employed. One is an Eshelby technique (see, e.g., [14,20–24]). Another is the finite element method (FEM) (e.g., [25–28]). The third approach uses Green's functions (e.g., [29–33]). In the Eshelby technique, the spontaneous strain is treated as an eigenstrain [34]. This approach offers a convenient way of analyzing problems where transformation deformation exists within one localized inclusionlike region in a large body. However, it is somewhat less convenient when multiple inclusionlike transformation zones are involved or the zone of spontaneous strain is a large fraction of the body being analyzed. FEM can be used effectively for geometries of arbitrary size and shape with single or multiple residual strain zones of a general configuration. However, FEM requires significant effort to cover the relevant parameter range and to obtain broad parametric characterization. The Green's function method is convenient and straightforward when used for simple transformation geometries. Hutchinson [29] solved the plane problem of a semi-infinite crack in an infinite, isotropic, linear elastic body with two transformed circular "spots" symmetrically located relative to the crack plane. Based on this solution, the transformation toughening problem of a zone with spontaneous strain surrounding the crack tip has been studied extensively (e.g., [30,31,33]). However, the results of that effort are only valid for problems with transformed zones that are *symmetrical* with respect to the crack plane. Additionally, Rose [32] represented the effect of both dilatant and deviatoric transformation strain components by a set of fundamental singular solutions including a force doublet, similar to the work of Love [35]. Using Rose's solution, Karihaloo and Andreasen [36] conducted a detailed study on transformation toughing. In addition, Li and Anderson [37] used a method similar to that of Rose [32] to obtain the solution for the effect of a cube of transformed material in an infinite, isotropic body where they used singular solutions for dislocations to characterize the results. From the above body of work, it is apparent that the Green's function method is convenient and easy to implement for the problem of transformation toughening in an isotropic solid. For this reason, we adopt Green's functions to address the more general transformation toughening problem associated with an anisotropic elastic solid. Such a situation arises in a cracked body that is a single crystal having an anisotropic lattice, and in which a stress-triggered martensitic phase transformation occurs, or in which ferroelastic behavior is enabled, perhaps by domain switching of twin variants. The present paper provides some of the basic analytical tools enabling the analysis of such phenomena.

Manuscript received May 18, 2011; final manuscript received April 23, 2012; accepted manuscript posted January 22, 2013; published online July 12, 2013. Assoc. Editor: Kenneth M. Liechti.

It is important to note that the planar methodology proposed here is derived from the concepts of a dislocation and a dislocation dipole, as used for the isotropic case by Li and Anderson [37]. To obtain our results, we use solutions for edge dislocations that have their Burgers vectors confined to the plane of the body, and that have no Burgers vector component in the transverse direction. Such dislocations are *not* used here as crystallographic defects, but are utilized for the convenience of obtaining the desired solutions for the transformation toughening problems we tackle. Consequently, our dislocations do not need to be consistent with conditions imposed by the symmetry of the lattice that real lattice defects would have to satisfy. Our dislocations, in dipole pairs, are used merely to represent the effects of *nuclei of transformation strain*, giving us fundamental elasticity solutions corresponding to given distributions of spontaneous strain.

The formulation is constructed using the following steps. First, Stroh formalism and displacement potentials for an edge dislocation in an infinite anisotropic plane are introduced in Sec. 2. Based on these results, the fundamental solutions for a transformation strain nucleus located within an infinite anisotropic elastic plane are derived in Sec. 3. Thereafter, a fundamental formulation for transformation toughening, namely, the interaction of a transformation strain nucleus with a semi-infinite crack in an anisotropic body is studied in Sec. 4. In Sec. 5, two representative examples of transformation toughening in an anisotropic body are studied by the Green's function method. Finally, conclusions are drawn in Sec. 6.

2 Stroh Formalism and Displacement Potential for an Edge Dislocation

2.1 Stroh Formalism. In a Cartesian coordinate system x_i $(i=1, 2, 3)$, the equations of linear infinitesimal elasticity are [38]

$$\sigma_{ij} = c_{ijkl}\varepsilon_{kl} \tag{2.1}$$

$$\varepsilon_{ij} = \frac{1}{2}\left(u_{i,j} + u_{j,i}\right) \tag{2.2}$$

$$\sigma_{ij,j} = 0 \tag{2.3}$$

where σ_{ij}, ε_{kl}, u_i, and c_{ijkl} $(i, j, k, l=1, 2, 3)$ are the stress tensor, the strain tensor, the displacement vector, and the elasticity tensor, respectively. A comma followed by an integer i indicates differentiation with respect to x_i. The elasticities satisfy the following symmetry relation:

$$c_{ijkl} = c_{jikl} = c_{ijlk} = c_{klij} \tag{2.4}$$

For planar behavior, where u_i $(i=1,2,3)$ depend on $x_1(=x)$ and $x_2(=y)$ only, the displacement vector $\mathbf{u}=[u_1\ u_2\ u_3]^T$ and the generalized stress function vector $\boldsymbol{\varphi}=[\phi_1\ \phi_1\ \phi_1]^T$ can be expressed as

$$\mathbf{u} = 2\,\mathrm{Re}[\mathbf{A}\mathbf{f}(z)], \quad \boldsymbol{\varphi} = 2\,\mathrm{Re}[\mathbf{B}\mathbf{f}(z)] \tag{2.5}$$

and the stress components as

$$\begin{aligned}\boldsymbol{\sigma}_1 &= [\,\sigma_{11}\quad \sigma_{21}\quad \sigma_{31}\,]^T = -\boldsymbol{\varphi}_{,y} = -2\,\mathrm{Re}[\mathbf{B}\mathbf{P}\mathbf{f}_{,z}(z)]\\ \boldsymbol{\sigma}_2 &= [\,\sigma_{12}\quad \sigma_{22}\quad \sigma_{32}\,]^T = \boldsymbol{\varphi}_{,x} = 2\,\mathrm{Re}[\mathbf{B}\mathbf{f}_{,z}(z)]\end{aligned} \tag{2.6}$$

Here

$$\mathbf{A} = [\,\mathbf{a}_1\quad \mathbf{a}_2\quad \mathbf{a}_3\,], \quad \mathbf{B} = [\,\mathbf{b}_1\quad \mathbf{b}_2\quad \mathbf{b}_3\,] \tag{2.7}$$

are complex constants, and we have functions given by

$$\begin{aligned}\mathbf{f}(\mathbf{z}) &= [f_1(z_1)\quad f_2(z_2)\quad f_3(z_3)\,]^T,\\ z_i &= x + p_i y, \quad \mathrm{Im}(p_i) > 0 \quad (i=1,2,3)\end{aligned} \tag{2.8}$$

where the superscript T indicates transposition, $f_i(z_i)$ $(i=1, 2, 3)$ are arbitrary analytic functions of z_i, and $i=\sqrt{-1}$. The notation $\mathbf{f}_{,z}(z)$ indicates that f_i is to be differentiated with respect to z_i, whereas $\boldsymbol{\varphi}_{,x}$ indicates partial differentiation of $\boldsymbol{\varphi}$ with respect to x, and $\boldsymbol{\varphi}_{,y}$ with respect to y. The column vectors $\mathbf{a}_i$ $(i=1, 2, 3)$ of matrix $\mathbf{A}$, and the entries in $\mathbf{P}=\mathrm{diag}\,[p_1\ p_2\ p_3]$ are determined by the following eigenrelation:

$$\left[\mathbf{Q} + p_i\left(\mathbf{R}+\mathbf{R}^T\right) + p_i^2\mathbf{T}\right]\mathbf{a}_i = \mathbf{0} \quad (i=1,2,3) \tag{2.9}$$

where $\mathbf{Q}$, $\mathbf{R}$, and $\mathbf{T}$ are 3×3 matrices whose components are

$$\mathbf{Q} = [c_{i1k1}], \quad \mathbf{R} = [c_{i1k2}], \quad \mathbf{T} = [c_{i2k2}] \tag{2.10}$$

Matrix $\mathbf{B}$ in (2.5) is related to matrix $\mathbf{A}$ in (2.5) by the following relationship:

$$\mathbf{B} = \mathbf{R}^T\mathbf{A} + \mathbf{T}\mathbf{A}\mathbf{P} \tag{2.11}$$

Matrices $\mathbf{A}$ and $\mathbf{B}$ also satisfy the following orthogonality relation if they are properly normalized:

$$\begin{bmatrix}\mathbf{A} & \overline{\mathbf{A}}\\ \mathbf{B} & \overline{\mathbf{B}}\end{bmatrix}\begin{bmatrix}\mathbf{B}^T & \mathbf{A}^T\\ \overline{\mathbf{B}}^T & \overline{\mathbf{A}}^T\end{bmatrix} = \begin{bmatrix}\mathbf{I} & 0\\ 0 & \mathbf{I}\end{bmatrix} \tag{2.12}$$

or, expressed in a different way,

$$\begin{aligned}\mathbf{A}\mathbf{B}^T + \overline{\mathbf{A}}\,\overline{\mathbf{B}}^T &= \mathbf{I} = \mathbf{B}\mathbf{A}^T + \overline{\mathbf{B}}\,\overline{\mathbf{A}}^T\\ \mathbf{A}\mathbf{A}^T + \overline{\mathbf{A}}\,\overline{\mathbf{A}}^T &= \mathbf{0} = \mathbf{B}\mathbf{B}^T + \overline{\mathbf{B}}\,\overline{\mathbf{B}}^T\end{aligned} \tag{2.13}$$

where $\mathbf{I}$ is the unit matrix. From (2.13), the Barnett–Lothe tensors are defined as

$$\mathbf{H} = 2i\mathbf{A}\mathbf{A}^T, \quad \mathbf{L} = -2i\mathbf{B}\mathbf{B}^T, \quad \mathbf{S} = i\left(2\mathbf{A}\mathbf{B}^T - \mathbf{I}\right) \tag{2.14}$$

where $\mathbf{H}$, $\mathbf{L}$, and $\mathbf{S}$ are real, and $\mathbf{H}$ and $\mathbf{L}$ are symmetric positive definite. They depend only on the material constants c_{ijkl}.

In the presence of material elastic anisotropy a separation into purely in-plane and purely out-of-plane deformation states may no longer be possible, i.e., in-plane stressing may induce out-of-plane strains and displacements, unless the plane of consideration is one of material symmetry. Since here we wish to consider a two-dimensional formulation, we will accept this limitation, bearing in mind that (i) we wish to preserve the simplicity of analysis associated with a crack that preserves the planar nature of the problem, and (ii) the formulation will provide insights on the effects of material anisotropy for such planar behavior.

2.2 Edge Dislocation. The displacement potentials for a dislocation characterized by the Burgers vector $\mathbf{b}=[\,b_1\quad b_2\quad b_3\,]^T = b[\cos\psi\quad \sin\psi\quad 0\,]^T$ of magnitude b, and also for a line force $\mathbf{e}=[e_1\ e_2\ e_3]^T$, colocated at the origin within an infinite plane solid, can be expressed in the form

$$\mathbf{f}_d(z) = \langle \ln z\rangle\mathbf{q} \tag{2.15}$$

where $\langle \ln z\rangle = \mathrm{diag}[\,\ln z_1\quad \ln z_2\quad \ln z_3\,]$, and the complex coefficient vector $\mathbf{q}=[q_1\ q_2\ q_3]^T$ is to be determined in terms of $\mathbf{b}$ and $\mathbf{e}$ by the displacement and force conditions

$$\oint_c d\mathbf{u} = \mathbf{b}, \quad \oint_c d\boldsymbol{\varphi} = \mathbf{e} \tag{2.16}$$

for any curve C enclosing the origin. Inserting (2.15) into (2.5) and then into (2.16) we get

$$\begin{bmatrix} \mathbf{A} & \overline{\mathbf{A}} \\ \mathbf{B} & \overline{\mathbf{B}} \end{bmatrix} \begin{bmatrix} \mathbf{q} \\ -\overline{\mathbf{q}} \end{bmatrix} = \frac{1}{2\pi i} \begin{bmatrix} \mathbf{b} \\ \mathbf{e} \end{bmatrix} \tag{2.17}$$

Using (2.12) we can solve for $\mathbf{q}$ as

$$\begin{aligned} \begin{bmatrix} \mathbf{q} \\ -\overline{\mathbf{q}} \end{bmatrix} &= \frac{1}{2\pi i} \begin{bmatrix} \mathbf{A} & \overline{\mathbf{A}} \\ \mathbf{B} & \overline{\mathbf{B}} \end{bmatrix}^{-1} \begin{bmatrix} \mathbf{b} \\ \mathbf{e} \end{bmatrix} = \frac{1}{2\pi i} \begin{bmatrix} \mathbf{B}^T & \mathbf{A}^T \\ \overline{\mathbf{B}}^T & \overline{\mathbf{A}}^T \end{bmatrix} \begin{bmatrix} \mathbf{b} \\ \mathbf{e} \end{bmatrix} \\ &= \frac{1}{2\pi i} \begin{bmatrix} \mathbf{B}^T\mathbf{b} + \mathbf{A}^T\mathbf{e} \\ \overline{\mathbf{B}}^T\mathbf{b} + \overline{\mathbf{A}}^T\mathbf{e} \end{bmatrix} \end{aligned} \tag{2.18}$$

If $\mathbf{e} = \mathbf{0}$, we obtain the dislocation solution

$$\mathbf{q} = \frac{1}{2\pi i}\mathbf{B}^T\mathbf{b} = \frac{1}{4\pi}\mathbf{B}^{-1}\mathbf{L}\mathbf{b} \tag{2.19}$$

Thus, substituting (2.19) into (2.15), we find that the displacement potential for an edge dislocation located at the origin within an infinite plane solid is

$$\mathbf{f}_d(z) = \frac{1}{4\pi}\langle \ln z \rangle \mathbf{B}^{-1}\mathbf{L}\mathbf{b} \tag{2.20}$$

It is easy to prove that the expressions $\mathbf{A}\langle * \rangle \mathbf{B}^{-1}$ and $\mathbf{B}\langle * \rangle \mathbf{B}^{-1}$ are independent of the factor introduced for normalization mentioned in conjunction with Eqs. (2.12) and (2.13), and are only dependent on the elastic material constants c_{ijkl}. Hence direct substitution of (2.20) into (2.5) uniquely determines the deformation and stress fields of a dislocation at the origin with Burgers vectors $\mathbf{b}$ in an infinite solid.

3 Fundamental Solution for a Transformation Strain Nucleus Located in an Infinite Plane Solid

In this section we seek the *Stroh formalism potential* for a transformation strain nucleus located in an infinite plane solid. These nuclei will be represented by superposition of edge dislocations.

3.1 Stroh Potential for a Transformation Strain Nucleus. Consider an infinitesimal element with an area dA $(= dx_0 dy_0)$, which undergoes an unconstrained transformation deformation with two *principal* strains ε_{x0} and ε_{y0} expressed in local *principal* coordinates x_0, y_0 as shown in Fig. 1. The origin of the local coordinate system x_0, y_0 lies at the location represented symbolically by z_0 in the global coordinate system x, y, and ψ is the orientation angle of the x_0 axis (associated with the *principal* strain ε_{x0}) with respect to the global x-coordinate axis. Note that $z_{0i} = x_0 + p_i y_0$. In view of the physical meaning of the edge dislocation, the region of infinitesimal transformation strain can be represented by an assembly of four dislocations, as shown in Fig. 1. Dislocations 1 and 3 form a dislocation dipole, as do dislocations 2 and 4. The two dipole systems are perpendicular to each other and lie around the point z_0. The Stroh potential for these four dislocations can be derived in a stepwise fashion, as described below.

3.1.1 Potential of Dipole 1-3 (Fig. 1). The potential in global coordinates for the dislocation dipole formed by dislocations *1 and 3* can be obtained by summing the contribution of the two

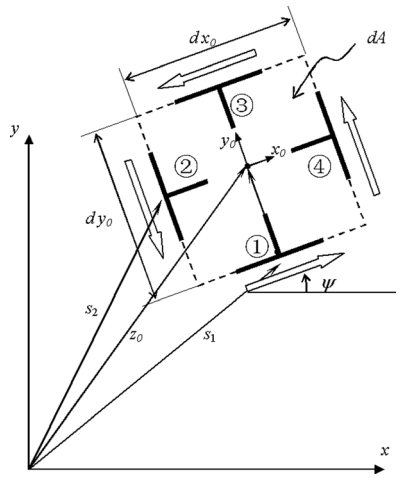

Fig. 1 An infinitesimal element with transformation strain located in an infinite plane solid

dislocations forming the dipole. Since the transformation zone is infinitesimal and the dipoles have opposite Burgers vectors, such a process can be carried out by differentiating the potential of dislocation 1 with respect to the coordinate vector from the center of the transformation zone to dislocation 1 and multiplying the result by the corresponding dipole length dy_0. The potential for dislocation 1 in Fig. 1 is

$$\mathbf{f}_{d1}(z) = \frac{1}{4\pi}\langle \ln(z - s_1) \rangle \mathbf{B}^{-1}\mathbf{L}\mathbf{b}_1 \tag{3.1}$$

where

$$\mathbf{b}_1 = \varepsilon_{x0} dx_0 \mathbf{n}(\psi), \quad \mathbf{n}(\psi) = [\cos\psi \quad \sin\psi \quad 0]^T \tag{3.2}$$

$$s_{1i} = z_{0i} + y_0(\sin\psi - p_i \cos\psi) \tag{3.3}$$

where y_0 is the magnitude of the distance from the center of the transformation zone to dislocation 1 when taken to be not infinitesimal. The potential of dislocation dipole 1-3 formed by dislocations 1 and 3 is then found from

$$\begin{aligned} \mathbf{f}_{\text{dipole}1-3} &= \frac{\partial \mathbf{f}_{d1}}{\partial y_0}_{|y_0=0} dy_0 \\ &= \frac{1}{4\pi}\varepsilon_{x0}\left\langle \frac{-\sin\psi + p\cos\psi}{(z - z_0)} \right\rangle \mathbf{B}^{-1}\mathbf{L}\mathbf{n}(\psi) dx_0 dy_0 \\ &= \frac{1}{4\pi}\varepsilon_{x0}\left\langle \frac{-\sin\psi + p\cos\psi}{(z - z_0)} \right\rangle \mathbf{B}^{-1}\mathbf{L}\mathbf{n}(\psi) dA \end{aligned} \tag{3.4}$$

3.1.2 Potential of Dipole 2-4 (Fig. 1). Similarly, in global coordinates, the potential for dislocation dipole 2-4 formed by dislocations *2 and 4* can be obtained by differentiating the potential of dislocation 2 with respect to x_0, and multiplying by dx_0, where x_0 is the magnitude of the distance from the center of the transformation zone to dislocation 2, when the distance is taken to be not infinitesimal. The potential for dislocation 2 is

$$\mathbf{f}_{d2}(z) = \frac{1}{4\pi}\langle \ln(z - s_2) \rangle \mathbf{B}^{-1}\mathbf{L}\mathbf{b}_2 \tag{3.5}$$

$$\mathbf{b}_2 = -\varepsilon_{y0} dy_0 \mathbf{m}(\psi), \quad \mathbf{m}(\psi) = [-\sin\psi \quad \cos\psi \quad 0]^T \tag{3.6}$$

$$s_{2i} = z_{0i} - x_0(\cos\psi + p_i \sin\psi) \tag{3.7}$$

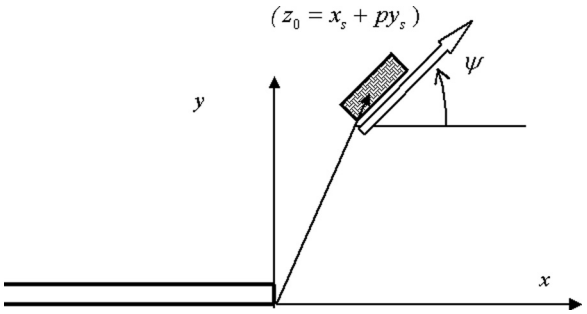

Fig. 2 A transformation strain nucleus interacting with a semi-infinite crack in an infinite body

The potential of dislocation dipole 2-4 is then given by

$$\begin{aligned}\mathbf{f}_{\text{dipole2-4}}(z) &= \frac{\partial \mathbf{f}_{d2}(z)}{\partial x_{0|x_0=0}} dx_0 \\ &= -\frac{1}{4\pi}\varepsilon_{y0}\left\langle \frac{\cos\psi + p\sin\psi}{(z-z_0)} \right\rangle \mathbf{B}^{-1}\mathbf{L}\mathbf{m}(\psi) dx_0 dy_0 \\ &= -\frac{1}{4\pi}\varepsilon_{y0}\left\langle \frac{\cos\psi + p\sin\psi}{(z-z_0)} \right\rangle \mathbf{B}^{-1}\mathbf{L}\mathbf{m}(\psi) dA \end{aligned} \tag{3.8}$$

Consequently, the potential of the *four-dislocation nucleus* in the global coordinate system is obtained by summing (3.4) and (3.8),

$$\mathbf{f}_0 = \mathbf{f}_{\text{dipole1-3}} + \mathbf{f}_{\text{dipole2-4}} \tag{3.9}$$

Therefore, the potential for a nucleus of transformation strain located at z_0 *in an infinite anisotropic solid is*

$$\begin{aligned}\mathbf{f}_0(z) = \frac{dA}{4\pi}\Bigg[&\varepsilon_{x0}\left\langle \frac{-\sin\psi + p\cos\psi}{(z-z_0)} \right\rangle \mathbf{B}^{-1}\mathbf{L}\mathbf{n}(\psi) \\ &-\varepsilon_{y0}\left\langle \frac{\cos\psi + p\sin\psi}{(z-z_0)} \right\rangle \mathbf{B}^{-1}\mathbf{L}\mathbf{m}(\psi)\Bigg] \end{aligned} \tag{3.10}$$

Solution (3.10) is the *fundamental solution for a nucleus of strain* obtained in this study.

4 Formulation of the Transformation Toughening Problem

It is assumed that the size of the transformation strain region is small compared with the crack length and other problem dimensions. Hence, in this section we will concentrate on the basic problem of a transformation strain nucleus interacting with a *semi-infinite* crack in an infinite plane.

4.1 Stroh Potential for a Transformation Strain Nucleus Interacting With a Semi-Infinite Crack. Consider a transformation strain nucleus as described above, located at point (x_s, y_s) so that its location is defined by the complex parameter z_0 which is now evaluated through $z_{0i} = x_s + p_i y_s$. The orientation angle is ψ, and the spot interacts with a semi-infinite crack occupying the negative half of the x axis and with its tip at the origin, as shown in Fig. 2. By the superposition principle, the problem shown in Fig. 2 can be decomposed into two subproblems shown in Figs. 3(*a*) and 3(*b*).

For convenience we express the second equation of (2.6) as

$$\boldsymbol{\sigma}_2 = \boldsymbol{\varphi}_{,x} = 2\text{Re}[\mathbf{B}\mathbf{f}_{,x}(z)] = 2\text{Re}[\mathbf{h}(z)], \quad \text{i.e.,} \quad \mathbf{h}(z) = \mathbf{B}\mathbf{f}_{,z}(z) \tag{4.1}$$

Using this notation, the subproblems in Fig. 3 can be solved as follows.

(i) Subproblem (*a*): The solution to this problem can be obtained from Eq. (3.10) by differentiation with respect to z so that the relevant function $\mathbf{h}$ is given by

$$\begin{aligned}\mathbf{h}_a(z) = -\frac{dA}{4\pi}\Bigg\{ &\varepsilon_{x0}\mathbf{B}\left\langle \frac{-\sin\psi + p\cos\psi}{(z-z_0)^2} \right\rangle \mathbf{B}^{-1}\mathbf{L}\mathbf{n}(\psi) \\ &-\varepsilon_{y0}\mathbf{B}\left\langle \frac{\cos\psi + p\sin\psi}{(z-z_0)^2} \right\rangle \mathbf{B}^{-1}\mathbf{L}\mathbf{m}(\psi)\Bigg\} \end{aligned} \tag{4.2}$$

(ii) Subproblem (*b*): To find the complex function $\mathbf{h}_b(z)$ for subproblem (*b*), we note from subproblem (*a*) that in an infinite plane, the traction on the x axis induced by the transformation strain nucleus according to Eq. (4.1) is stated as

$$\boldsymbol{\sigma}_{20}(x) = [\,\sigma_{12} \quad \sigma_{22} \quad \sigma_{32}\,]^T = \boldsymbol{\varphi}_{0_{,x}}(x) = 2\text{Re}[\mathbf{h}_a(x)] \tag{4.3}$$

To ensure a traction-free crack for the problem in Fig. 2, the tractions on the crack surface of subproblem (*b*) must be $-\boldsymbol{\sigma}_{20}(x)$. The general solution for this subproblem is [39,40]

$$\mathbf{h}_b(z) = -\frac{1}{2\pi}\frac{1}{\sqrt{z}}\int_{-\infty}^{0} \frac{\boldsymbol{\sigma}_{20}(t)\sqrt{|t|}}{(t-z)} dt \tag{4.4}$$

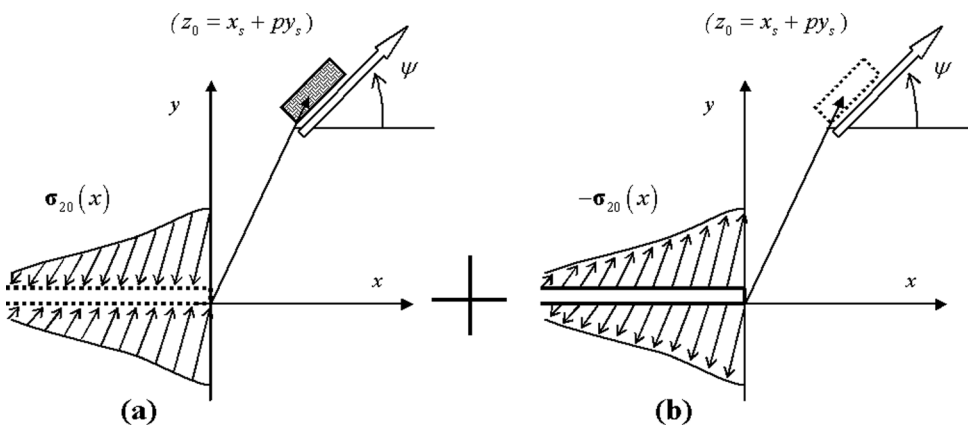

Fig. 3 Two subproblems forming the decomposition of the original problem in Fig. 2. (*a*) Transformation strain nucleus in an infinite plane without a crack. (*b*) Application on the semi-infinite crack surfaces of the negative of the tractions due to the transformation strain nucleus.

Substituting (4.2) into (4.3) and then (4.3) into (4.4), we obtain the solution of subproblem (b) as

$$\mathbf{h}_b(z)=\frac{dA}{(2\pi)^2}\frac{1}{\sqrt{z}}\int_{-\infty}^{0}\mathrm{Re}\left[\begin{Bmatrix}\varepsilon_{x0}\mathbf{B}\left\langle\frac{-\sin\psi+p\cos\psi}{(t-z_0)^2}\right\rangle\mathbf{B}^{-1}\mathbf{Ln}(\psi)\\ -\varepsilon_{y0}\mathbf{B}\left\langle\frac{\cos\psi+p\sin\psi}{(t-z_0)^2}\right\rangle\mathbf{B}^{-1}\mathbf{Lm}(\psi)\end{Bmatrix}\right]\times\frac{\sqrt{|t|}}{(t-z)}dt$$

$$=-\frac{dA}{(2\pi)^2}\frac{1}{\sqrt{z}}\int_{0}^{\infty}\mathrm{Re}\left[\begin{Bmatrix}\varepsilon_{x0}\mathbf{B}\left\langle\frac{-\sin\psi+p\cos\psi}{(t+z_0)^2}\right\rangle\mathbf{B}^{-1}\mathbf{Ln}(\psi)\\ -\varepsilon_{y0}\mathbf{B}\left\langle\frac{\cos\psi+p\sin\psi}{(t+z_0)^2}\right\rangle\mathbf{B}^{-1}\mathbf{Lm}(\psi)\end{Bmatrix}\right]\times\frac{\sqrt{t}}{(t+z)}dt \tag{4.5}$$

Consequently, by superposing the solutions of the above two subproblems together, the solution for the problem of a transformation strain nucleus interacting with a semi-infinite crack shown in Fig. 2 is finally obtained as

$$\mathbf{h}(z)=\mathbf{h}_a(z)+\mathbf{h}_b(z) \tag{4.6}$$

From (2.6), the stress field is obtained as

$$\boldsymbol{\sigma}_2=\boldsymbol{\varphi}_{,x}=2\mathrm{Re}[\mathbf{Bf}_{,x}(z)]=2\mathrm{Re}[\mathbf{Bf}_{,z}(z)]=2\mathrm{Re}[\mathbf{h}(z)] \tag{4.7}$$

$$\boldsymbol{\sigma}_1=-\boldsymbol{\varphi}_{,y}=-2\mathrm{Re}[\mathbf{Bf}_{,y}(z)]=-2\mathrm{Re}[\mathbf{BPf}_{,z}(z)]=-2\mathrm{Re}[\mathbf{BPB}^{-1}\mathbf{h}(z)] \tag{4.8}$$

4.2 Influence Function for the Calculation of Stress Intensity Factors. According to the traditional stress intensity factors' definition, the stress intensity factors at the crack tip due to the presence of the transformation strain nucleus can be computed as follows:

$$\begin{aligned}d\mathbf{K}&=\lim_{y=0,x\to0^+}\sqrt{2\pi x}\boldsymbol{\sigma}_2\\&=\lim_{y=0,x\to0^+}\sqrt{2\pi x}2\mathrm{Re}[\mathbf{h}(z)]\\&=\lim_{x\to0^+}\sqrt{2\pi x}2\mathrm{Re}[\mathbf{h}_a(x)+\mathbf{h}_b(x)]\\&=\lim_{x\to0^+}\sqrt{2\pi x}2\mathrm{Re}[\mathbf{h}_b(x)]\end{aligned} \tag{4.9}$$

Inserting (4.5) into (4.9) gives

$$d\mathbf{K}=\lim_{x\to0^+}\sqrt{2\pi x}2\mathrm{Re}\left\{\frac{-dA}{(2\pi)^2}\frac{1}{\sqrt{x}}\int_0^{\infty}\mathrm{Re}\left[\begin{Bmatrix}\varepsilon_{x0}\mathbf{B}\left\langle\frac{-\sin\psi+p\cos\psi}{(t+z_0)^2}\right\rangle\mathbf{B}^{-1}\mathbf{Ln}(\psi)\\ -\varepsilon_{y0}\mathbf{B}\left\langle\frac{\cos\psi+p\sin\psi}{(t+z_0)^2}\right\rangle\mathbf{B}^{-1}\mathbf{Lm}(\psi)\end{Bmatrix}\right]\frac{\sqrt{t}}{(t+x)}dt\right\}$$

$$=-\frac{dA}{\pi\sqrt{2\pi}}\mathrm{Re}\left\{\int_0^{\infty}\mathrm{Re}\left[\begin{Bmatrix}\varepsilon_{x0}\mathbf{B}\left\langle\frac{-\sin\psi+p\cos\psi}{(t+z_0)^2}\right\rangle\mathbf{B}^{-1}\mathbf{Ln}(\psi)\\ -\varepsilon_{y0}\mathbf{B}\left\langle\frac{\cos\psi+p\sin\psi}{(t+z_0)^2}\right\rangle\mathbf{B}^{-1}\mathbf{Lm}(\psi)\end{Bmatrix}\right]\frac{\sqrt{t}}{t}dt\right\}$$

$$=\frac{-dA}{2\sqrt{2\pi}}\mathrm{Re}\left[\varepsilon_{x0}\mathbf{B}\left\langle\frac{(-\sin\psi+p\cos\psi)}{z_0^{\frac{3}{2}}}\right\rangle\mathbf{B}^{-1}\mathbf{Ln}(\psi)-\varepsilon_{y0}\mathbf{B}\left\langle\frac{(\cos\psi+p\sin\psi)}{z_0^{\frac{3}{2}}}\right\rangle\mathbf{B}^{-1}\mathbf{Lm}(\psi)\right] \tag{4.10}$$

where $d\mathbf{K}=[\,dK_{\mathrm{II}}\quad dK_{\mathrm{I}}\quad dK_{\mathrm{III}}\,]^T$ are infinitesimal contributions to the stress intensity factors for mode II, mode I, and mode III, representing in-plane shear, tension, and antiplane shear, respectively, relative to the positive x axis near the crack tip.

5 Examples: Tetragonal Crystals

The anisotropic elastic constitutive law for tetragonal crystalline materials, e.g., tetragonal zirconia, can be expressed using six independent material constants as

$$\begin{bmatrix}c_{11}&c_{12}&c_{13}&0&0&0\\c_{12}&c_{11}&c_{13}&0&0&0\\c_{13}&c_{13}&c_{33}&0&0&0\\0&0&0&c_{44}&0&0\\0&0&0&0&c_{44}&0\\0&0&0&0&0&c_{66}\end{bmatrix}\begin{bmatrix}\varepsilon_{11}\\\varepsilon_{22}\\\varepsilon_{33}\\2\varepsilon_{23}\\2\varepsilon_{13}\\2\varepsilon_{12}\end{bmatrix}=\begin{bmatrix}\sigma_{11}\\\sigma_{22}\\\sigma_{33}\\\sigma_{23}\\\sigma_{13}\\\sigma_{12}\end{bmatrix} \tag{5.1}$$

where the x_3 axis is the tetragonal direction and other two axes are taken to be the in-plane x_1 and x_2 coordinate directions. Note that in tetragonal symmetry the elastic constant c_{66} is independent of the other elasticities; in contrast to transverse isotropy, where $c_{66}=(c_{11}-c_{12})/2$. Whereas transverse isotropy around the x_3 axis leads to plane strain elasticity problems in the x_1–x_2 plane that can be solved by methods valid for isotropic materials, this is not the case for tetragonal symmetry, and Stroh formalism becomes necessary. With the elastic matrix given by Eq. (5.1), we then find

$$\mathbf{Q}=\begin{bmatrix}c_{11}&0&0\\0&c_{66}&0\\0&0&c_{44}\end{bmatrix},\quad\mathbf{R}=\begin{bmatrix}0&c_{12}&0\\c_{66}&0&0\\0&0&0\end{bmatrix},\quad\mathbf{T}=\begin{bmatrix}c_{66}&0&0\\0&c_{11}&0\\0&0&c_{44}\end{bmatrix} \tag{5.2}$$

Substituting (5.2) into (2.9) we get

$$\begin{bmatrix}c_{11}+c_{66}p^2&(c_{12}+c_{66})p&0\\(c_{12}+c_{66})p&c_{66}+c_{11}p^2&0\\0&0&c_{44}(1+p^2)\end{bmatrix}\mathbf{a}=0 \tag{5.3}$$

and the characteristic equation

$$\det\begin{bmatrix} c_{11}+c_{66}p^2 & (c_{12}+c_{66})p & 0 \\ (c_{12}+c_{66})p & c_{66}+c_{11}p^2 & 0 \\ 0 & 0 & c_{44}(1+p^2) \end{bmatrix}=0 \tag{5.4}$$

From (5.4) we may find the three complex characteristic roots [Im $(p_i)>0$]

$$p_1=\frac{1}{2}\left(\sqrt{2-\eta}+i\sqrt{2+\eta}\right),$$
$$p_2=\frac{1}{2}\left(-\sqrt{2-\eta}+i\sqrt{2+\eta}\right),\quad p_3=i \tag{5.5}$$

where $\eta=(c_{11}^2-c_{12}^2-2c_{12}c_{66})/c_{11}c_{66}$, and the pair of matrices $\mathbf{A}_*$ and $\mathbf{B}_*$ is given in a non-normalized form by

$$\mathbf{A}_*=\begin{bmatrix} -\dfrac{p_1^2c_{11}+c_{66}}{p_1^2c_{11}-c_{12}} & -\dfrac{p_2^2c_{11}+c_{66}}{p_2^2c_{11}-c_{12}} & 0 \\ \dfrac{p_1(c_{12}+c_{66})}{p_1^2c_{11}-c_{12}} & \dfrac{p_2(c_{12}+c_{66})}{p_2^2c_{11}-c_{12}} & 0 \\ 0 & 0 & 1 \end{bmatrix}$$
$$\mathbf{B}_*=\begin{bmatrix} -c_{66}p_1 & -c_{66}p_2 & 0 \\ c_{66} & c_{66} & 0 \\ 0 & 0 & ic_{44} \end{bmatrix} \tag{5.6}$$

Matrix $\mathbf{L}$ can then be directly evaluated as [38]

$$\mathbf{L}=\left[\mathrm{Re}\left[i\mathbf{A}_*\mathbf{B}_*^{-1}\right]\right]^{-1}=\begin{bmatrix} (c_{12}+c_{11})\beta & 0 & 0 \\ 0 & (c_{12}+c_{11})\beta & 0 \\ 0 & 0 & c_{44} \end{bmatrix} \tag{5.7}$$

with $\beta=\sqrt{\dfrac{c_{66}(c_{11}-c_{12})}{c_{11}(c_{11}+c_{12}+2c_{66})}}$.

5.1 Example 1: Interaction Between an Infinite Crack and a Transformed Spot Having an Area Change. Here we wish to study an infinite crack interacting with a small, circular cylindrical transformation strain region whose cross-sectional area changes, but has no deviatoric component to the transformation (Fig. 4). A similar case was investigated within the framework of isotropic elasticity by McMeeking and Evans [20].

If the radius of the cylinder is much smaller than its distance from the crack tip ($R \ll r$), and since $\varepsilon_{x0}=\varepsilon_{y0}=\varepsilon_0$, then from (4.10) we obtain as the contribution to the stress intensity factors due to the zone as

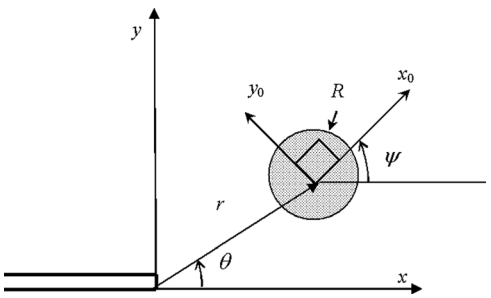

Fig. 4 A circular transformation strain zone in an anisotropic solid with a semi-infinite crack

$$\Delta\mathbf{K}=\begin{bmatrix}\Delta K_{II}\\ \Delta K_{\mathrm{I}}\\ \Delta K_{\mathrm{III}}\end{bmatrix}=-\frac{\pi R^2\varepsilon_0}{2\sqrt{2\pi}}\mathrm{Re}\begin{bmatrix}\mathbf{B}\left\langle\dfrac{(-\sin\psi+p\cos\psi)}{z_0^{\frac{3}{2}}}\right\rangle\mathbf{B}^{-1}\mathbf{Ln}(\psi)\\ -\mathbf{B}\left\langle\dfrac{(\cos\psi+p\sin\psi)}{z_0^{\frac{3}{2}}}\right\rangle\mathbf{B}^{-1}\mathbf{Lm}(\psi)\end{bmatrix} \tag{5.8}$$

By directly substituting $\mathbf{B}_*$, $\mathbf{L}$, $\mathbf{n}$, and $\mathbf{m}$ into (5.8), it simplifies to

$$\Delta K=\begin{bmatrix}\Delta K_{\mathrm{II}}\\ \Delta K_{\mathrm{I}}\\ \Delta K_{\mathrm{III}}\end{bmatrix}=-\frac{\pi R^2(c_{11}+c_{12})\beta\varepsilon_0}{2\sqrt{2\pi}}\mathrm{Re}\begin{bmatrix}\left(\dfrac{p_2}{z_{02}^{\frac{3}{2}}}+\dfrac{p_1}{z_{01}^{\frac{3}{2}}}\right)\\ -\left(\dfrac{1}{z_{02}^{\frac{3}{2}}}+\dfrac{1}{z_{01}^{\frac{3}{2}}}\right)\\ 0\end{bmatrix} \tag{5.9}$$

where

$$x_s=r\cos\theta,\quad y_s=r\sin\theta$$
$$(z_{01})^{\frac{3}{2}}=(x_s+p_1y_s)^{\frac{3}{2}}=r^{\frac{3}{2}}(\cos\theta+p_1\sin\theta)^{\frac{3}{2}}$$
$$(z_{02})^{\frac{3}{2}}=(x_s+p_2y_s)^{\frac{3}{2}}=r^{\frac{3}{2}}(\cos\theta+p_2\sin\theta)^{\frac{3}{2}} \tag{5.10}$$

or

$$\Delta K_{\mathrm{I}}=\frac{\pi R^2(c_{11}+c_{12})\beta\varepsilon_0}{2\sqrt{2\pi}}\mathrm{Re}\left[\left(\frac{1}{z_{02}^{\frac{3}{2}}}+\frac{1}{z_{01}^{\frac{3}{2}}}\right)\right]$$
$$\Delta K_{\mathrm{II}}=-\frac{\pi R^2(c_{11}+c_{12})\beta\varepsilon_0}{2\sqrt{2\pi}}\mathrm{Re}\left[\left(\frac{p_2}{z_{02}^{\frac{3}{2}}}+\frac{p_1}{z_{01}^{\frac{3}{2}}}\right)\right] \tag{5.11}$$

Since the solution (5.11) is independent of the Stroh matrices $\mathbf{A}$ and $\mathbf{B}$, and the generalized stress function $\mathbf{f}(z)$, it depends *only* on the relevant material parameters, including how they influence the eigenvalues controlling z_{01} and z_{02}. Therefore Eq. (5.11) can be specialized to the isotropic solution by use of

$$c_{11}=c_{33}=\frac{E(1-\nu)}{(1+\nu)(1-2\nu)},\quad c_{44}=c_{66}=\frac{E}{2(1+\nu)},$$
$$c_{12}=c_{13}=\frac{E\nu}{(1+\nu)(1-2\nu)} \tag{5.12}$$

in which case $z_{01}=z_{02}=z_0=x_s+iy_s=re^{i\theta}$. As a result, Eq. (5.11) gives

$$\Delta K_{\mathrm{I}}=\frac{\pi R^2(c_{11}+c_{12})\beta\varepsilon_0}{\sqrt{2\pi}}\mathrm{Re}\left[\frac{1}{z_0^{\frac{3}{2}}}\right]=\frac{E\varepsilon_0}{(1-\nu^2)}\frac{\pi R^2}{2\sqrt{2\pi}}\frac{\cos\frac{3\theta}{2}}{r^{\frac{3}{2}}}$$
$$\Delta K_{\mathrm{II}}=-\frac{\pi R^2(c_{11}+c_{12})\beta\varepsilon_0}{\sqrt{2\pi}}\mathrm{Re}\left[\frac{i}{z_0^{\frac{3}{2}}}\right]=-\frac{E\varepsilon_0}{(1-\nu^2)}\frac{\pi R^2}{2\sqrt{2\pi}}\frac{\sin\frac{3\theta}{2}}{r^{\frac{3}{2}}} \tag{5.13}$$

This outcome is consistent with the results of McMeeking and Evans [20].

It can be seen in Eq. (5.9) to Eq. (5.13) that (ΔK_{I}, ΔK_{II}) are proportional to $r^{-\frac{3}{2}}$ for both isotropic and anisotropic material models. On the other hand, the influence of the angle θ on the stress intensity factor for the anisotropic and isotropic cases is different. We assess this by a normalization of the stress intensity factors, designed to produce a result that is unity at $\theta=0$ in the case of ΔK_{I} when the isotropic material is considered. The results are from (5.13) for the isotropic case

$$\Delta\widetilde{K}_{\mathrm{I}}=\frac{2\sqrt{2\pi}(1-\nu^2)r^{\frac{3}{2}}}{E\varepsilon_0\pi R^2}\Delta K_{\mathrm{I}}=\cos\frac{3}{2}\theta$$
$$\Delta\widetilde{K}_{\mathrm{II}}=\frac{2\sqrt{2\pi}(1-\nu^2)r^{\frac{3}{2}}}{E\varepsilon_0\pi R^2}\Delta K_{\mathrm{II}}=-\sin\frac{3}{2}\theta \tag{5.14}$$

and from (5.11) for the anisotropic case

$$\Delta\widetilde{K}_{\mathrm{I}}=\frac{\sqrt{2\pi}r^{\frac{3}{2}}\Delta K_{\mathrm{I}}}{\pi R^2(c_{11}+c_{12})\beta\varepsilon_0}=\frac{1}{2}\mathrm{Re}\left[\frac{1}{(\cos\theta+p_2\sin\theta)^{\frac{3}{2}}}+\frac{1}{(\cos\theta+p_1\sin\theta)^{\frac{3}{2}}}\right]$$
$$\Delta\widetilde{K}_{\mathrm{II}}=\frac{\sqrt{2\pi}r^{\frac{3}{2}}\Delta K_{\mathrm{II}}}{\pi R^2(c_{11}+c_{12})\beta\varepsilon_0}=-\frac{1}{2}\mathrm{Re}\left[\frac{p_2}{(\cos\theta+p_2\sin\theta)^{\frac{3}{2}}}+\frac{p_1}{(\cos\theta+p_1\sin\theta)^{\frac{3}{2}}}\right] \tag{5.15}$$

The contrasting dependence on θ in Eqs. (5.14) and (5.15) makes it clear that the anisotropy influences how a transformed spot experiencing area change produces an alteration to the stress intensity factor that depends on the angular location of the spot relative to the crack tip. To bring this point into greater focus, we have obtained numerical results for the case of an area changing transformation in zirconia to demonstrate the influence of the angle θ on the stress intensity factors. The elastic constants of tetragonal zirconia in units of GPa are $c_{11}=327$, $c_{12}=100$, $c_{13}=62$, $c_{33}=264$, $c_{44}=59$, $c_{66}=64$ [41]. This gives the values $p_1=1.937i$, $p_2=0.5161i$, and $\beta=0.2829$. The resulting variation

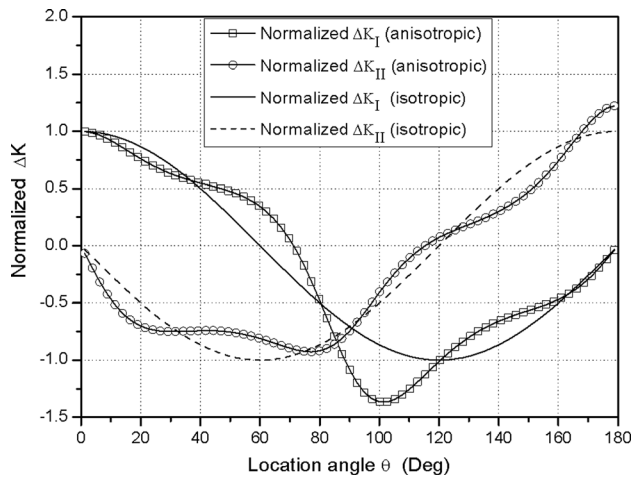

Fig. 5 Normalized stress intensity factor contributions due to a cylindrical transformation strain zone at angle θ

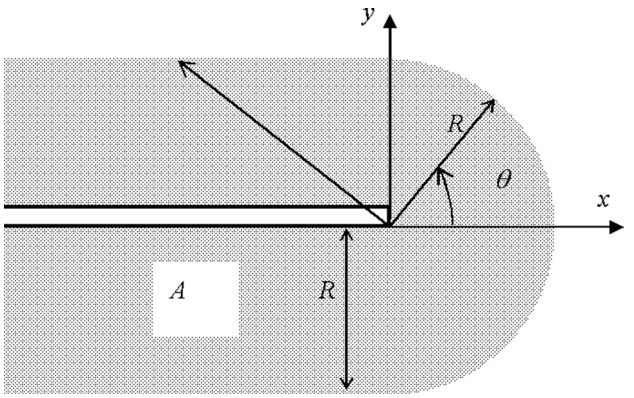

Fig. 6 A crack is enclosed by a transformed wake

of the stress intensity factors with the angle θ for both anisotropic and isotropic materials is plotted in Fig. 5. It can be seen that anisotropy influences the variation, and makes a modest, though significant, difference to the stress intensities produced by the spot.

5.2 Example 2: A Semi-Infinite Crack Enclosed by a Transformed Wake. Consider a semi-infinite crack enclosed by a transformed wake A as shown in Fig. 6. Suppose the radius of the transformed circular area in front of crack tip is R, the wake is infinite, extending to $x=-\infty$, and the transformation involves area change without a deviatoric component ($\varepsilon_{x0}=\varepsilon_{x0}=\varepsilon_0$). Note that there is no out-of-plane transformation strain. We assume that the elastic properties of the transformed material are identical to those of the untransformed material that surrounds it, a reasonable assertion in the case of a purely area changing transformation without change of orientation of the tetragonality. Note that the assumption of homogeneous elasticity is suspect if the crystallography changes, as in a phase change from monoclinic to tetragonal. Inserting $\mathbf{B}_*$, $\mathbf{L}$, $\mathbf{n}$, and $\mathbf{m}$ into (4.10), we obtain

$$d\mathbf{K}=\frac{-\varepsilon_0 dA}{2\sqrt{2\pi}}\mathrm{Re}\left[\mathbf{B}\left\langle\frac{(-\sin\psi+p\cos\psi)}{z_0^{\frac{3}{2}}}\right\rangle\mathbf{B}^{-1}\mathbf{L}\mathbf{n}(\psi)-\mathbf{B}\left\langle\frac{(\cos\psi+p\sin\psi)}{z_0^{\frac{3}{2}}}\right\rangle\mathbf{B}^{-1}\mathbf{L}\mathbf{m}(\psi)\right]$$
$$=\frac{-(c_{11}+c_{12})\beta\varepsilon_0 dA}{2\sqrt{2\pi}}\mathrm{Re}\begin{bmatrix}\frac{p_2}{z_{02}^{3/2}}+\frac{p_1}{z_{01}^{3/2}}\\-\left(\frac{1}{z_{02}^{3/2}}+\frac{1}{z_{01}^{3/2}}\right)\\0\end{bmatrix} \tag{5.16}$$

By use of the Green's function method, the changes to the stress intensity factors due to the transformed wake zone can be evaluated by performing integration on the zone A as

$$\Delta\mathbf{K}=\frac{-(c_{11}+c_{12})\beta\varepsilon_0}{2\sqrt{2\pi}}\int_A\mathrm{Re}\begin{bmatrix}\left(\frac{p_2}{z_{02}^{3/2}}+\frac{p_1}{z_{01}^{3/2}}\right)\\-\left(\frac{1}{z_{02}^{3/2}}+\frac{1}{z_{01}^{3/2}}\right)\\0\end{bmatrix}dA \tag{5.17}$$

By performing a straightforward integration, we can simplify Eq. (5.17) to

$$\Delta K_{\mathrm{I}} = -\frac{(c_{11}+c_{12})\beta\varepsilon_0\sqrt{R}}{\sqrt{2\pi}} \times \mathrm{Re}\left[\begin{array}{l} 2\left(\dfrac{1}{\sqrt{p_1}}+\dfrac{1}{\sqrt{-p_1}}+\dfrac{1}{\sqrt{p_2}}+\dfrac{1}{\sqrt{-p_2}}\right) \\ -\displaystyle\int_{-\frac{\pi}{2}}^{\frac{\pi}{2}}\left[\frac{1}{(\cos\theta+p_1\sin\theta)^{\frac{3}{2}}}+\frac{1}{(\cos\theta+p_2\sin\theta)^{\frac{3}{2}}}\right]d\theta \end{array}\right]$$

$$\Delta K_{\mathrm{II}} = -\frac{(c_{11}+c_{12})\beta\varepsilon_0\sqrt{R}}{\sqrt{2\pi}} \times \mathrm{Re}\left[\begin{array}{l} 2\left(\sqrt{-p_1}-\sqrt{p_1}+\sqrt{-p_2}-\sqrt{p_2}\right) \\ +\displaystyle\int_{-\frac{\pi}{2}}^{\frac{\pi}{2}}\left[\frac{p_1}{(\cos\theta+p_1\sin\theta)^{\frac{3}{2}}}+\frac{p_2}{(\cos\theta+p_2\sin\theta)^{\frac{3}{2}}}\right]d\theta \end{array}\right]$$

$$\Delta K_{\mathrm{III}} = 0 \tag{5.18}$$

When we substitute the characteristic roots obtained in example 1 into Eq. (5.18), namely $p_1 = 1.937i$, $p_2 = 0.5161i$, we obtain

$$\Delta K_{\mathrm{I}} = -2.267\frac{(c_{11}+c_{12})\beta\varepsilon_0\sqrt{R}}{\sqrt{2\pi}} \qquad \Delta K_{\mathrm{II}} = 0 \tag{5.19}$$

As in the isotropic case, a transformation involving in-plane expansion of the material reduces the stress intensity factor [20,30]. Note that Eq. (5.19) can be specialized to the isotropic case through use of Eq. (5.12). We then obtain

$$\Delta K_{\mathrm{I}} = -0.452\frac{E\varepsilon_0\sqrt{R}}{1-\nu^2} \tag{5.20}$$

Now consider a dilatant transformation that includes a transformation strain in the out-of-plane direction, letting the volume strain of the transformation be ε_v^T. After the out-of-plane strain of the transformation has been suppressed to maintain plane strain, we find that in the isotropic case $\varepsilon_0 = (1+\nu)\varepsilon_v^T/3$. Thus, Eq. (5.20) becomes

$$\Delta K_{\mathrm{I}} = -0.151\frac{E\varepsilon_v^T\sqrt{R}}{1-\nu} \tag{5.21}$$

This differs from the result of McMeeking and Evans [20] because the shape of the zone used here is not the same as that used by McMeeking and Evans [20]. The zone used here is a semicircle ahead of the crack tip, whereas that used by McMeeking and Evans [20] extends further beyond the crack tip for the same zone width. This difference in zone shape fully explains the difference between Eq. (5.21) and the result of McMeeking and Evans [20], where the coefficient 0.151 in Eq. (5.21) is replaced by 0.22. While the shape of the transformation zone is particularly simple in the case analyzed by us to obtain Eq. (5.19) to (5.21), in principle the formulation can be used for more complex zone shapes, such as those controlled by a transformation criterion of an appropriate form, e.g., a critical hydrostatic stress as used by McMeeking and Evans [20] and Budiansky et al. [30].

6 Conclusions

Fundamental solutions for a transformation strain nucleus located in an infinite plane, and in a plane containing a semi-infinite crack, have been derived in the framework of plane anisotropic elasticity theory. Two simple examples for tetragonal zirconia are studied to demonstrate that the formulation paves the way to the possibility of a systematic study of transformation stress problems in anisotropic solids.

Acknowledgment

This work was partially supported by Ph.D. Programs Foundation of Ministry of Education of China, the Natural Science Foundation of Shaanxi Province of China, and the Fundamental Research Funds for the Central Universities.

References

[1] Garvie, R. C., Hannink, R. H. J., and Pascoe, R. T., 1975, "Ceramic Steel?," Nature, **258**, pp. 703–704.
[2] Claussen, N., 1976, "Fracture Toughness of Al_2O_3 With an Unstabilized ZrO_2 Dispersed Phase," J. Am. Ceram. Soc., **59**, pp. 49–51.
[3] Gupta, T. K., Bechtold, J. H., Kuznicki, R. C., Cadoff, L. H., and Rossing, B. R., 1977, "Stabilization of Tetragonal Phase in Polycrystalline Zirconia," J. Mater. Sci., **12**, pp. 2421–2426.
[4] Hannink, R. H. J., 1978, "Growth Morphology of the Tetragonal Phase in Partially Stabilized Zirconia," J. Mater. Sci., **13**, pp. 2487–2496.
[5] Evans, A. G., and Heuer, A. H., 1980, "Review—Transformation Toughening in Ceramics: Martensitic Transformations in Crack-Tip Stress Fields," J. Am. Ceram. Soc., **63**, pp. 241–248.
[6] Lange, F. F., 1982, "Transformation Toughening—Part 2, Contribution to Fracture Toughness," J. Mater. Sci., **17**, pp. 235–239.
[7] Munz, D., and Fett, T., 1998, *Ceramics—Mechanical Properties, Failure Behaviour, Material Selection* (Springer Series in Material Sciences), Springer, Berlin.
[8] Hannink, R. H. J., Kelly, P. M., and Muddle, B. C., 2000, "Transformation Toughening in Zirconia-Containing Ceramics," J. Am. Ceram. Soc., **83**, pp. 461–487.
[9] Rauchs, G., Fett, T., Munz, D., and Oberacker, R., 2001, "Tetragonal-to-Monoclinic Phase Transformation in CeO_2-Stabilized Zirconia Under Uniaxial Loading," J. Eur. Ceram. Soc., **21**, pp. 2229–2241.
[10] Rauchs, G., Fett, T., Munz, D., and Oberacker, R., 2002, "Tetragonal-to-Monoclinic Phase Transformation in CeO_2-Stabilized Zirconia Under Multiaxial Loading," J. Eur. Ceram. Soc., **22**, pp. 841–849.
[11] Kelly, P. M., and Rose, L. R. F., 2002, "The Martensitic Transformation in Ceramics—Its Role in Transformation Toughening," Prog. Mater. Sci., **47**, pp. 463–557.
[12] Magnani, G., and Brillante, A., 2005, "Effect of the Composition and Sintering Process on Mechanical Properties and Residual Stresses in Zirconia-Alumina Composites," J. Eur. Ceram. Soc., **25**, pp. 3383–3392.
[13] Claussen, N., Ruehle, M., and Heuer, A. H., 1984, "Science and Technology of Zirconia II," *Advances in Ceramics*, American Ceramic Society, Columbus, OH, Vol. 12.
[14] Yang, W., and Zhu, T., 1998, "Switch-Toughening of Ferroelectrics Subjected to Electric Fields," J. Mech. Phys. Solids, **46**, pp. 291–311.
[15] Wang, J., Shi, S. Q., Chen, L., Q. Li, Y., and Zhang, T. Y., 2004, "Phase Field Simulations of Ferroelectric/Ferroelastic Polarization Switching," Acta Mater., **52**, pp. 749–764.
[16] Jones, J. L., Salz, C. R. J., and Hoffman, M., 2005, "Ferroelastic Fatigue of a Soft PZT Ceramic," J. Am. Ceram. Soc., **88**, pp. 2788–2792.
[17] Jones, J. L., and Hoffman, M., 2006, "R-Curve and Stress-Strain Behavior of Ferroelastic Ceramics," J. Am. Ceram. Soc., **89**, pp. 3721–3727.
[18] Jones, J. L., Motahari, S. M., Varlioglu, M., Lienert, U., Bernier, J. V., Hoffman, M., and Uestuendag, E., 2007, "Crack Tip Process Zone Domain Switching in a Soft Lead Zirconate Titanate Ceramic," Acta Mater., **55**, pp. 5538–5548.
[19] Pojprapai, S., Jones, J. L., Studer, A. J., Russell, J., Valanoor, N., and Hoffman, M., 2008, "Ferroelastic Domain Switching Fatigue in Lead Zirconate Titanate Ceramics," Acta Mater., **56**, pp. 1577–1587.
[20] McMeeking, R. M., and Evans, A. G., 1982, "Mechanics of Transformation-Toughening in Brittle Materials," J. Am. Ceram. Soc., **65**, pp. 242–246.
[21] Yi, S., and Gao, S., 2000, "Fracture Toughening Mechanism of Shape Memory Alloys Due to Martensite Transformation," Int. J. Solids Struct., **37**, pp. 5315–5327.
[22] Yi, S., Gao, S., and Shen, L. X., 2001, "Fracture Toughening Mechanism of Shape Memory Alloys Under Mixed-Mode Loading Due to Martensite Transformation," Int. J. Solids Struct., **38**, pp. 4463–4476.
[23] Li, Z. H., and Yang, L. H., 2002, "The Application of the Eshelby Equivalent Inclusion Method for Unifying Modulus and Transformation Toughening," Int. J. Solids Struct., **39**, pp. 5225–5240.
[24] Fischer, F. D., and Boehm, H. J., 2005, "On the Role of the Transformation Eigenstrain in the Growth or Shrinkage of Spheroidal Isotropic Precipitates," Acta Mater., **53**, pp. 367–374.
[25] Hom, C. L., and McMeeking, R. M., 1990, "Numerical Results for Transformation Toughening in Ceramics," Int. J. Solids Struct., **26**, pp. 1211–1223.
[26] Zeng, D., Katsube, N., and Soboyejo, W. O., 1999, "Simulation of Transformation Toughening of Heterogeneous Materials With Randomly Distributed Transforming Particles by Hybrid FEM," Comput. Mech., **23**, pp. 457–465.
[27] Zeng, D., Katsube, N., and Soboyejo, W. O., 2004, "Discrete Modeling of Transformation Toughening in Heterogeneous Materials," Mech. Mater., **36**, pp. 1057–1071.

[28] Vena, P., Gastaldi, D., Contro, R., and Petrini, L., 2006, "Finite Element Analysis of the Fatigue Crack Growth Rate in Transformation Toughening Ceramics," Int. J. Plast., **22**, pp. 895–920.
[29] Hutchinson, J. W., 1974, "On Steady Quasi-Static Crack Growth," Harvard University Report DEAP S-8 (AFOSR-TR-74-1042).
[30] Budiansky, B., Hutchinson, J. W., and Lambropoulos, J. C., 1983, "Continuum Theory of Dilatant Transformation Toughness in Ceramics," Int. J. Solids Struct., **19**, pp. 337–355.
[31] Lambropoulos, J. C., 1986, "Effect of Nucleation on Transformation Toughening," J. Am. Ceram. Soc., **69**, pp. 218–222.
[32] Rose, L. R. F., 1987, "The Mechanics of Transformation Toughening," Proc. R. Soc. London Ser. A, **412**, pp. 169–197.
[33] Tsukamoto, H., and Kotousov, A., 2006, "Transformation Toughening in Zirconia-Enriched Composites: Micromechanical Modeling," Int. J. Fract., **139**, pp. 161–168.
[34] Mura, T., 1987, *Micromechanics of Defects in Solids*, Martinus Nijhoff, Dordrecht, The Netherlands.
[35] Love, A. E. H., 1927, *Mathematical Theory of Elasticity*, Cambridge University Press, Cambridge, UK.
[36] Karihaloo, B. L., and Andreasen, J. H., 1996, *Mechanics of Transformation Toughening and Related Topics*, Elsevier, Amsterdam.
[37] Li, Q., and Anderson, P. M., 2001, "A Compact Solution for the Stress Field From a Cuboidal Region With a Uniform Transformation Strain," J. Elast., **64**, pp. 237–245.
[38] Ting, T. C. T., 1996, *Anisotropic Elasticity: Theory and Application*, Oxford University Press, Oxford, UK.
[39] Hirth, J. P., and Wagoner, R. H., 1976, "Elastic Fields of Line Defects in a Cracked Body," Int. J. Solids Struct., **12**, pp. 117–123.
[40] Ma, L., Lu, T. J., and Korsunsky, A. M., 2006, "Vector J-Integral Analysis of Crack Interaction With Pre-Existing Singularities," ASME J. Appl. Mech., **73**, pp. 876–883.
[41] Kisi, E. H., and Howard, C. J., 1998, "Elastic Constants of Tetragonal Zirconia Measured by a New Powder Diffraction Technique," J. Am. Ceram. Soc., **81**, pp. 1682–1684.